Extended Abstracts of the 2010 International Conference on Solid State Devices and Materials, Tokyo, 2010, pp371-372

Enhanced Device Performance of AlGaN/GaN MOSHEMT with Thermal Oxidation

Shenghou Liu[1], Jinyan Wang[1], Rumin Gong[1], Zhihua Dong[1], Min Yu[1], C. P. Wen[1], Chunhong Zeng[2], Yong Cai[2], Baoshun Zhang[2]

[1]Institute of Microelectronics, Peking University, Beijing 100871, China
Phone: +86-10-6275-2579 E-mail: shliu2009@sinano.ac.cn;jywang@ ime.pku.edu.cn; ntgrm@hotmail.com; zhhdong@ime.pku.edu.cn ;yum@ime.pku.edu.cn;cpwen@ieee.org;
[2]Suzhou Institute of Nano-tech and Nano-bionics,
Chinese Academy of Sciences, Suzhou 215125, China
Phone: +86-512-6287-2517 E-mail: chzeng2007@sinano.ac.cn;ycai2008@sinano.ac.cn;bszhang2006@sinano.ac.cn

1. Introduction

The superior properties of GaN-based heterojunction materials have made AlGaN/GaN HEMTs promising contenders for high-power, high temperature and high-frequency applications[1]. While the conventional Schottky AlGaN/GaN HEMTs still suffer from many problems, such as large gate leakage current[2], low breakdown voltage, current collapse[3], which may constrain the power handing capacity of the transistors.

The thermal oxidation could improve the performance of AlGaN/GaN heterostructure, reported in the previous literatures[4-6]. In this article, we adopted this technique to fabricate the AlGaN/GaN MOSHEMT, and investigated systematically its electric characteristics. Our results show that this simple and low cost technique could not only effectively reduce leakage current and trap density, but also significantly increase the breakdown voltage.

2. General Instructions

Experiments

The process of MOSHEMT was described as follows. The AlGaN/GaN heterostructure was grown by MOCVD on (0001) sapphire substrate. The mesa isolation was accomplished by Inductive coupling plasma (ICP) etching. Ti/Al/Ni/Au Ohmic contact was deposited by electron beam evaporation (EBE), followed by rapid thermal annealing (RTA) at 900℃ for 30s in N_2 ambient. Then, the samples were oxidized from 400℃ to 600℃ for 30min in pure O_2 ambient, respectively. Finally, Ni/Au metal gate was formed by EBE. With almost the same processing, except for the thermal annealing of samples, a Schottky HEMT with identical geometry was also prepared as a comparison. The electric characteristics of both devices were measured by Keithley 4200 Semiconductor Characterization System.

Results and discussion

The gate leakage current of MOSHEMT at different oxidation temperatures and Schottky HEMT was shown in Fig.1. The reverse gate leakage current of the MOSHEMT at the oxidation temperature of 450℃ shows the lowest value, which is four orders of magnitude lower than that of the Schottky HEMT at V_{gs}=-10 V.

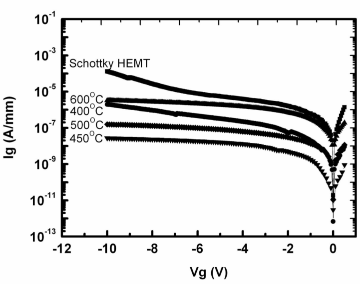

Fig. 1 the gate leakage current of MOSHEMT at different oxidation temperatures and Schottky HEMT as a function of gate voltage

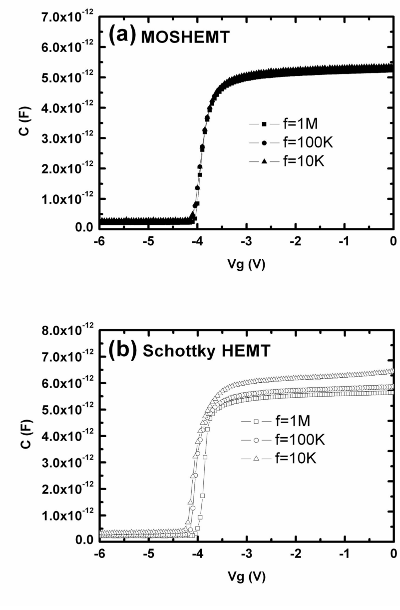

Fig. 2 Typical C-V characteristics of MOSHEMT (oxidized at 450℃)(a) and Schottky HEMT (b) measured at 1MHz, 100kHz and 10kHz

The typical C-V characteristics of the Schottky HEMT and MOSHEMT at 1MHz, 100KHz and 10KHz frequency were shown in Fig.2. In Fig.2 (b), a strong frequency dispersion of the Schottky structure capacitance is observed. While for the MOS structure, shown in Fig.2 (a), there is no noticeable frequency dispersion, which indicates a significant reduction of the interface trap of the MOS structure after the thermal oxidation. The trap density, according to the eq. (1)[7],

$$n_{\mathrm{t}} \sim n_{10\mathrm{kHz}} - n_{1\mathrm{MHz}} = \int C_{10\mathrm{kHz}}\,\mathrm{d}V - \int C_{1\mathrm{MHz}}\,\mathrm{d}V \qquad (1)$$

was reduced by 80% for MOSHEMT, comparing to Schottky HEMT.

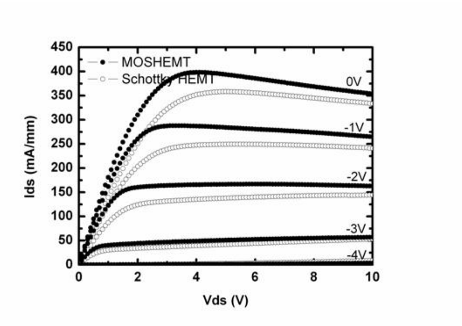

Fig. 3 Measured I-V output characteristics of the MOSHEMT (oxidized at 450℃) and the Schottky HEMT

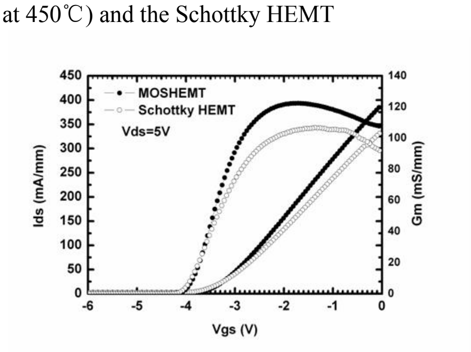

Fig. 4 Measured transfer and transconductance characteristics of the MOSHEMT (oxidized at 450℃) and the Schottky HEMT

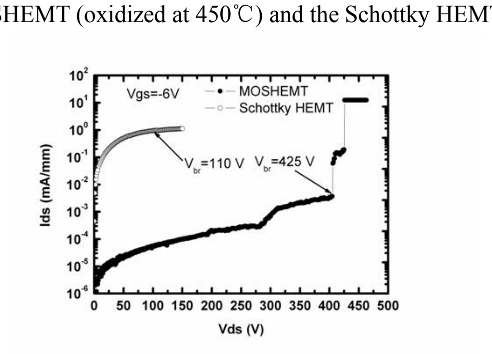

Fig. 5 the breakdown properties of MOSHEMT (oxidized at 450℃) and Schottky HEMT, at pinch-off state

The drain–source current (I_{DS}) as a function of the drain–source voltage (V_{DS}) of the Schottky HEMT and MOSHEMT is shown in Fig.3. At a V_{gs} of 0V, the saturation drain current of MOSHEMT is 398mA/mm, which is 11% higher than that of the Schottky HEMT, 357mA/mm.

The measured transfer characteristic and transconductance versus V_{GS} at V_{DS} =5V are shown in fig.4 for Schottky HEMT and MOSHEMT. The maximum transconductance in the MOSHEMT is 122mS/mm, and the threshold voltage is -3.34V. While for the Schottky HEMT, the maximum transconductance is 106mS/mm, and the threshold voltage is -3.25V. The threshold voltage almost maintains the same characteristics.

Both devices' pinch-off (with gate voltage of -6V) breakdown voltage was measured, as shown in Fig. 5. MOSHEMT has an 425V breakdown voltage, which is almost four times that of the Schottky HEMT, 110V. The almost four-times increase in V_{br}, coupled with a higher g_m, indicates MOSHEMT's greatly enhanced power handling capability than the Schottky HEMT.

3. Conclusions

In summary, the electric properties of AlGaN/GaN MOSHEMT with thermal oxidization in O_2 ambient was investigated, which demonstrates four orders of magnitude lower reverse gate leakage current, 80% lower interface trap density, and four times higher breakdown voltage as compared to its conventional Schottky HEMT counterpart. Furthermore, this MOS HEMT exhibits higher saturation drain current and peak transconductance. All the results show that AlGaN/GaN MOSHEMT with this simple and low cost processing, thermal oxidation, has a great potential for high power microwave power amplifier applications.

Acknowledgements

The work is supported by the National Natural Science Foundation of China (Nos. 60406004, 60890193, 60736033). The authors wish to acknowledge Nano Fabrication Facility and Platform for Characterization & Test, Suzhou Institute of Nano-tech and Nano-bionics, Chinese Academy of Science.

References

[1] Tsu-Yi Wu, Shun-Kuan Lin, Po-Wen Sze, Jian-Jiun Huang, Wei-Chi Chien, Chih-Chun Hu, Ming-Ji Tsai, and Yeong-Her Wang, IEEE Trans. Electron Devices **56** (2009) 2911.

[2] E. J. Miller, X. Z. Dang, and E. T. Yu, J. Appl. Phys. **88** (2000) 5951.

[3] J. A. Mittereder, S. C. Bibari, P. B. Klein, J. A. Roussos, D. S. Katzer, D. F. Storm, D. D. Koleske, A. E. Wickenden, and R. L.Henry, **83** (2003) 1650.

[4] F. Roccaforte, F. Giannazzo, F. Iucolano, C. Bongiorno, and V Raineri, J. Appl. Phys. **106** (2009) 023703.

[5] Chang Min Jeon, and Jong-Lam Lee, Appl. Phys. Lett. **82** (2003) 4301.

[6] X. L. Wang, D. G. Zhao, J. Chen, X. Y. Li, H. M. Gong, and H. Yang, Appl. Surf. Sci. **252** (2006) 8706.

[7] P. Kordoš, D. Gregušová, R. Stoklas, Š. Gaži, and J. Novák, Solid-State Electron. **52** (2008) 973.